Catalysis Science & Technology

Accepted Manuscript

ROYAL SOCIETY OF CHEMISTRY

www.rsc.org/catalysis

Morphological Investigations of Nanostructured V_2O_5 over Graphene Used for the ODHP Reaction: From Synthesis to Physiochemical Evaluations

Moslem Fattahi[1,2], Mohammad Kazemeini[1*], Farhad Khorasheh[1], Ali Morad Rashidi[3]

1. Department of Chemical and Petroleum Engineering, Sharif University of Technology, Azadi Avenue, P.O. Box 11365-9465, Tehran, Iran
2. Department of Chemical Engineering, Abadan Faculty of Petroleum Engineering, Petroleum University of Technology, Abadan, Iran
3. Nanotechnology Research Center, Tehran, Iran

Corresponding Author: Mohammad Kazemeini, Department of Chemical and Petroleum Engineering, Sharif University of Technology, Tehran, Iran

Address: Azadi Avenue, Sharif University of Technology, Tehran, Iran

Tel.: +98 21 6616 5425

Fax: +98 21 6602 2853

E-mail: kazemini@sharif.edu

Abstract

Oxidative dehydrogenation of propane (ODHP) in a fixed bed reactor over synthesized vanadia nanocatalysts was investigated physicochemically. Several vanadium pentoxide (V_2O_5) nanostructures including rod-, belt-, tube-, needle- and flower-likes were successfully synthesized via the reflux and hydrothermal processes utilizing different templates such as; monoamine, diamine, aromatic and alcoholic amines. Morphologies of the obtained products found to be sensitive to the types of templates used. Nano-rods obtained were of 1.4μm in length and about 97nm in width while the VO_2(B) nanotubes were of about 76nm average diameter and upto 1.2μm long. The diameters of the V_2O_5 nanotubes varied between 60-120nm with lengths upto 5μm. In this venue, the as-synthesized vanadium nanostructures with amines doped over graphene with 1:1 molar ratio of V:C prepared both through the reflux and hydrothermal methods. The surface morphologies determined by the scanning electron microscope (SEM). The structure of the prepared samples was then characterized utilizing the XRD, BET/BJH, FTIR, UV-vis and TGA techniques. Amongst, materials understudied, bulk catalyst of V_2O_5 prepared with dodecylamine and V_2O_5 synthesized by aniline over graphene were shown to be the most active catalysts for the ODHP reaction. The reactor test conditions of 450°C, feed of C_3H_8/Air molar ratio of 0.5 and the total feed flow rate of 60mL/min over the vanadium on graphene resulted in 53.93% selectivity for the propylene at 47.02% propane conversion after 6h; at the end of reaction. It was revealed that, under these conditions the cracking of the propane or propylene along with the CO_x formation as the side reaction occurred. Moreover, the effects of different reaction temperatures as well as propane to air ratio on propane conversion and product selectivities upon the two optimized catalysts designated as V-DDA and V-A-G were investigated.

Keywords: Oxidative dehydrogenation, Nanostructure, Vanadium pentoxide, Propane, Graphene, Amine

1. Introduction

Propylene is an important link between relatively cheap and abundant natural gas and many petrochemicals and intermediates such as propylene oxide, acrylonitrile and isopropyl alcohol. The conversion of light alkanes to their corresponding olefins was the subject of many

investigations over the last two decades. This was due to a worldwide increase in demand for light olefins. Instead the propane catalytic dehydrogenation (*i.e.;* the conventional method) was more selective than the established processes even though, it suffered from thermodynamic limitations, high-energy consumptions, side pyrolysis reactions as well as coke deposition in the system [1]. On the other hand, the dehydrogenation of propane in the presence of oxygen presented a feasible alternative. However, industrialization of this process has not been completely realized due to the fact that the most appropriate catalytic system has not yet been determined [1,2].

The first large-scale commercial plant of the STAR process® with oxidative dehydrogenation process is yet to be realized for the Egyptian Propylene & Polypropylene Company (EPPC) at Port Said in Egypt. Uhde Company shall built a turnkey plant producing 350,000 metric tons of propylene annually, with subsequent further processing into polypropylene including all associated off-sites and utility sections [3]. The acronym STAR stands for 'STeam Active Reforming', through which the catalytic dehydrogenation process took place in the presence of steam. The catalyst chosen to be a special platinum/tin complex fixed on a zinc aluminate support. Operation with steam reduced the partial pressure of the hydrocarbons and supposedly led to a higher propane equilibrium conversion rate. This meant that, the reaction could take place at higher absolute pressures of near 6bars reducing the investment costs and energy consumptions due to a planned raw gas compression [4]. Moreover, the reduced carbon deposits on the catalyst led to a less frequent regeneration cycle as a result [3,4]. Main reactions under the ODHP conditions were provided by the followings:

$$C_3H_8 + 0.5O_2 \longrightarrow C_3H_6 + H_2O \quad (1)$$

$$C_3H_8 + (2 + 1.5x)O_2 \longrightarrow 3CO_x + 4H_2O \quad (2)$$

$$C_3H_6 + (1.5 + 1.5x)O_2 \longrightarrow 3CO_x + 3H_2O \quad (3)$$

$$C_3H_8 + (1 + 0.5x)O_2 \longrightarrow C_2H_4 + CO_x + 2H_2O \quad (4)$$

$$C_3H_6 + (0.5 + 0.5x)O_2 \longrightarrow C_2H_4 + CO_x + H_2O \quad (5)$$

Most of the catalytic systems for the ODHP described in the open literature were based on the transition metal oxides with vanadia acting as such species. For propane conversion to propylene

via the ODHP process, supported vanadium oxide catalysts were reported as the most active and selective materials [2]. This was due to the vanadium ability to provide lattice oxygen for hydrogen removal from alkanes. A previous study in the literature revealed that, supported vanadium catalysts were more active in oxidative dehydrogenation (ODH) reactions with surface VO_x coverage in the sub-monolayer region [2]. A number of studies dealt with the effect of support and preparation method for vanadia supported materials [5,6]. V_2O_5 supported on TiO_2 was a well-established catalyst used in many industrial processes however, it was demonstrated to be a promising catalyst for the ODHP process [7]. In order to improve the catalytic behavior of vanadia-titania system various additives were examined and the most common ones determined to be oxides of potassium, phosphorous, tungsten and niobium [8]. An important and promising area of research in metal-free catalysts was that of the nanostructured carbons, and in particular carbon nanotubes (CNTs). Recent reports revealed an outstanding performance of nano-scale carbon materials in the ODH of hydrocarbons [9]. Both the inferior selectivity and the yield of alkenes retarded the industrial application of the ODH technology despite outstanding advantages of the oxidative pathway compared with non-oxidative processes for alkene production [10]. CNTs were promising catalysts for the ODH of ethylbenzene at a lower temperature and without excess supply of steam. Lately it was shown that, the CNTs with surface modification had a high potential for the activation of lower hydrocarbons [11]. The applications of the CNTs as catalysts attracted much interests in the catalysis community due to their unique porous microstructure and chemical properties. These materials exhibited excellent thermal conductivity, high surface area, and high thermal and chemical stabilities. Furthermore, carbon was also active and selective for catalytic oxidation reactions (*e.g.*; ODH of ethylbenzene to styrene [12]) most of which were highly exothermic. The energy released to the catalyst surface caused the catalytic activity or selectivity to decline since the thermal conductivity of the active catalysts and/or the normally used supports was rather low. This problem was solved by employing supports possessing higher thermal conductivity such as; CNTs, β-SiC, Si_3N_4, and BN [13] leading the heat from the catalyst surface to the reactor walls. In a different investigation, vanadium oxide-carbon nanotube composites were prepared by annealing a mixture of CNTs and V_2O_5 powder in air above the melting point of vanadium oxide. Such nanocomposites were synthesized by coating the surface of nitric acid-treated CNTs with vanadic acid. However, only a few works were reported on the use of the CNTs or other

carbonaceous materials to catalyze the ODH of light hydrocarbons [11,14]. Liu et al. [11] reported the application of the CNTs as catalysts in the ODH of 1-butene to butadiene. The catalytic performance of the CNTs was remarkably high, stable, and superior to that of the activated carbon and iron oxide. Characterizations of the CNTs before and after the reaction were made to test the hypothesis that, the oxygen functional groups were the active sites for the ODH reaction. The vanadium oxide nanotubes (VO_x-NTs) were especially interesting since vanadium oxides widely applied in electrochemical devices as well as catalytic applications. The VO_x-NTs synthesized in a rheological phase reaction followed by self-assembling process nonetheless, it was found that, there were residual organic templates left in the as-synthesized such species, endangering their desired properties [15].

Vanadia based catalysts showed high activity in various partial oxidation and oxidative dehydrogenation reactions of hydrocarbons. The higher reactivity of propylene in comparison to propane in oxidation reactions resulted in a fast consecutive propylene combustion limiting the product yield. A wider variety of catalysts and support materials nevertheless, investigated in the ODHP reaction.

In the case of the ODH reactions, catalysts under development exhibited high yields of olefins at high selectivities. This proved to be a challenging task due to the tendency of both the alkanes and olefins to produce CO and CO_2, depending on the nature of the catalyst [5,10,12,16]. In the past decade V_2O_5 gels were extensively studied [17]. More recently a way to synthesize vanadium oxide nanotubes (VO_x-NTs) by sol-gel reaction of a vanadium alkoxide with a primary amine or diamine, followed by a hydrothermal treatment was developed [18]. Nanostructured transition metal oxides represented a unique class of materials because of their redox activity relating to interesting electrochemical and catalytic properties. Recent advances in the sol-gel synthesis using organic molecules as structure-directing templates when combined with hydrothermal treatments provided appropriate methods for preparing meso-structured metal oxides. In particular, the application of such synthesis approached vanadium oxides possessing a rather huge variety of structures [19].

In this paper, means to synthesize nanostructures from the crystalline V_2O_5 and different amines as the reducing agent were reported. It was shown that, the amines were reasonable candidates to control the texture and morphology of the prepared materials. Here, synthesis of the vanadium nanostructures in the form of nano-rod, -tube, -needle and -flower types utilizing the V_2O_5 as the

source of the vanadium as well as propylamine, dodecylamine, aniline and diethanolamine as the reducing agents were investigated. This approach constituted a different strategy for preparing nano-structures of inorganic solids. Moreover, the obtained vanadium nanomaterials hybridized with graphene to provide catalysts with high conversion and selectivity towards propylene production.

2. Experimental

2.1. Catalysts preparation

The graphene nano-sheets were grown on copper foil by catalytic decomposition in a Quartz tube furnace system employing the CVD method. Before they were loaded into the furnace, the copper foils were pretreated by a 25% acetic acid solution and mixed up using a magnetic stirrer for several hours. Then, these foils were filtered from the acid solution and washed with deionized water until the pH of them reached neutral (*i.e.*, value of 7). Finally, the soaked copper foils were dried in vacuum oven at 90°C for 2h. Then, the CVD method involving methane and hydrogen gasses under vacuum condition of 10m-Torr to grow graphene utilized. The furnace was heated with a 3mL/min flow of hydrogen at temperature of 1050°C. After 40min of heating, the copper foils annealed under a flow of 35mL/min of methane introduced for a graphene growth time of 15min. A quick quenching after growth was applied while the methane and hydrogen gas flow continued throughout. Afterwards, copper particles were removed by purification treatment. Such purification included the process of using 50% HCl at 40°C with a magnetic stirrer for 16h. Then, the content of the flask was filtered under vacuum and washed out by distillated water reaching to pH of 7. Next, the filter cake was dried in a vacuum oven at 40°C for 8h. The details of the aforementioned experimental procedure and the in-house production by this research team were presented in the open literature [20,21]. To eliminate the amorphous carbon, graphene samples were calcined under air atmosphere at 400^{o}C for 2h.

Vanadium pentoxide (V_2O_5) (supplied by the Aldrich Chemicals Co.) was used as a vanadium source. Moreover, the organics reagents, propylamine, dodecylamine, benzylamine, aniline and diethanolamine utilized as templates. Bulk vanadium nanostructures synthesized with two consecutive steps of the reflux and hydrothermal methods. A mixture of V_2O_5 and different amines in the molar ratio of V/Amine=1:1 including propylamine (CH_3-$(CH_2)_2$-NH_2), dodecylamine (CH_3-$(CH_2)_{11}$-NH_2), aniline (C_6H_5-NH_2) and diethanolamine ((CH_2CH_2OH)-NH-

($OHCH_2CH_2$)) were dissolved in 200mL of ethanol at 90°C under vigorous stirring for 120min. This solution and 100mL of distilled water were transferred into a round-bottom flask of the reflux setup. The resulting suspension was introduced into a Teflon-lined steel autoclave while the temperature was set at 180°C for 48h. The resulting precipitate filtered and washed to get neutralized. This precipitate was then washed with a solution of ethanol and n-hexane to remove organic residues and then dried at 100°C for 24h to produce different vanadium oxide nanostructures. The black color of the powder suggested that some V^{5+} reduced to V^{4+} by decomposition of the organic compound [22]. The samples were subsequently calcined at 500°C for 2h under nitrogen and then air atmospheres, respectively. The resulting catalysts prepared by the reflux and then hydrothermal methods were designated as V-PA, V-DDA, V-A and V-DEA utilizing propylamine, dodecylamine, aniline and diethanolamine as the reducing agents, respectively.

The hybrid catalysts prepared by the reflux and hydrothermal methods consisted of V_2O_5, the above mentioned different amines and graphene, in carbon to vanadium to amine (C:V:Amine) molar ratio of 1:1:1. These were dissolved in 200mL of ethanol at 90°C under vigorous stirring for 120min. Other unit operations including the; reflux, hydrothermal, washing, drying and calcination were all the same as those employed for preparation of different bulk vanadium nanostructure materials. The resulting prepared hybrid catalysts were designated as V-PA-G, V-DDA-G, V-A-G and V-DEA-G indicating the prepared composite of vanadium and graphene with propylamine, dodecylamine, aniline and diethanolamine, respectively.

2.2. Catalyst characterization techniques

The catalysts were characterized by the FESEM, XRD, TGA/DTA, FTIR, ASAP and nitrogen porosimetry as well as the UV-Vis diffuse reflectance spectroscopy. Field Emission Scanning Electron Microscope (FESEM) images were obtained with a Hitachi S-4160 device. Gold was used as a conductive material for sample coating. Powder X-ray diffraction (XRD) measurements were conducted using standard powder diffraction procedure carried out with a STOE Analytical X-ray diffractometer (Cu k_α radiation, λ=1.5406Å). Data were collected for 2θ between 3-120° with a step size of 0.08°. The thermal analysis including; Thermo Gravimetric Analysis (TGA) and Differential Scanning Calorimetry (DSC) performed under air atmosphere with a heating rate of 5°C/min using a thermal analyzer TGA/DSC, METTLER, Japan from

room temperature up to 600°C. Subsequently, the FTIR analyses were performed and recorded on an ABB Bomem MB-100 spectrophotometer. FTIR spectra were obtained from KBr pellets taken from 4000 to 400cm^{-1} with a resolution of 4cm^{-1}. The pore size, textural properties and specific surface area of the catalysts were measured by nitrogen adsorption-desorption at -196^{o}C using the ASAP apparatus, model 2010 (Belsorp mini II manufactured by the BEL-Japan). The samples were initially degassed under vacuum at 200^{o}C for 12h. The BET/BJH methods were utilized for measuring the specific surface area, total pore volume, and average pore diameter. The UV-Visible spectroscopy was performed by the AvaSpec-2048Tec (For DRS & PL spectrum) with light source of AvaLightDH-S (providing the DRS spectrum) equipped with a diffusion reflectance accessory. UV-Vis spectra were measured in the range of 200-1100nm. In addition, 20-30mg of the powdered material was necessary to fill up the sample cup.

2.3. Experimental rig

Catalyst performance tests were carried out in a conventional tubular fixed-bed quartz reactor. A schematic of the utilized experimental setup displayed in Figure 1. The reactor was 14mm in diameter and 70cm long. It was placed in an electrical furnace equipped with a temperature controller to maintain the reactor temperature to within $\pm$1^{o}C of the desired set point using thermocouples placed both on the internal as well as external surface of the reactor. The catalyst loading was 0.5g mixed with 0.5g quartz beads for all ODHP experiments. Nitrogen, air and propane were all more than 99.9% in purity. The reactor was purged at room temperature with nitrogen for 2h. The reactor temperature was then increased to the desired value with a temperature ramp of 5^{o}C/min. The reaction temperature was performed at 450^{o}C. Air and propane gas flow rates were controlled by Brooks mass flow controllers. The exit gases were analyzed for the light hydrocarbons. The amounts of CO and CO_2 were determined through an online (Agilent model) gas chromatograph equipped with both TCD and FID detectors. In a typical experiment, product samples were analyzed after the start of the run when stable conditions achieved.

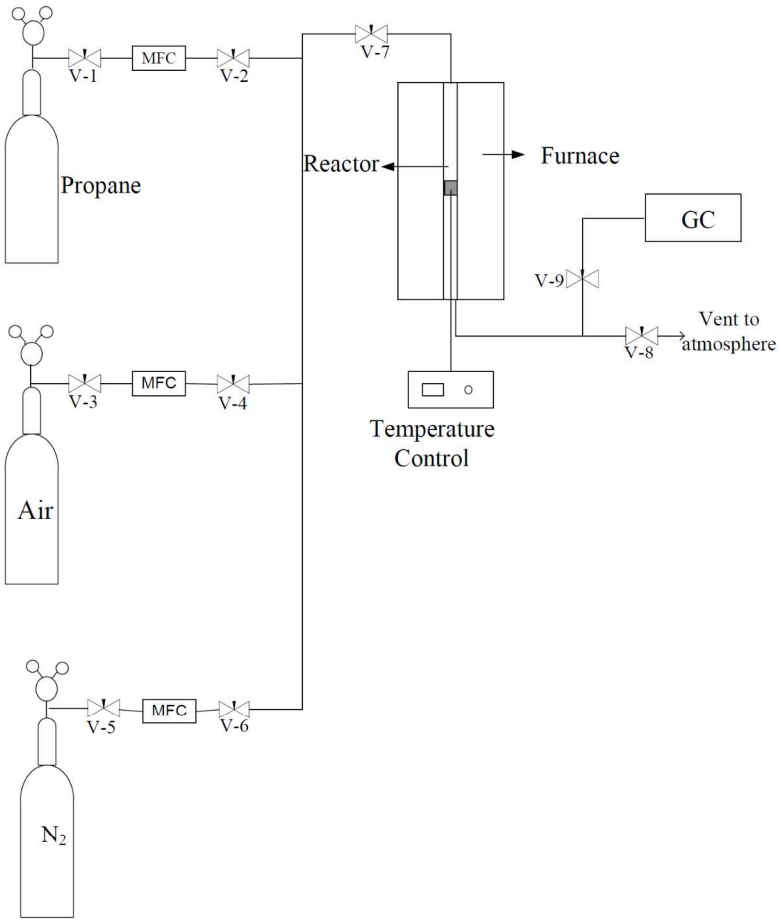

Figure 1: Schematic of the experimental apparatus utilized in the current research

Propane conversion, product selectivities and propylene yield were defined as follows:

$$Propane\ Conversion\ (\%) = \frac{\sum_i \left(\frac{n_i}{3}\right)[F_i]_{out} - \left[F_{C_3H_8}\right]_{out}}{\sum_i \left(\frac{n_i}{3}\right)[F_i]_{out}} \times 100 \quad (6)$$

$$Selectivity\ for\ component\ i\ (\%) = \frac{\left(\frac{n_i}{3}\right)[F_i]_{out}}{\sum_i \left(\frac{n_i}{3}\right)[F_i]_{out} - \left[F_{C_3H_8}\right]_{out}} \times 100 \quad (7)$$

$$Propylene\ Yield\ (\%) = \frac{Propane\ Conversion \times Selectivity\ of\ Propylene}{100} \quad (8)$$

where i included all the components containing carbon atoms in the exit gas stream, n_i was the number of carbon atoms of component i and F_i was the corresponding molar flowrate.

3. Catalysts characterization results

3.1. FESEM micrographs

The FESEM micrographs of mixtures of the V_2O_5 treated with propylamine (V-PA) displayed in Figure 2a exhibited that, the synthesized material was made of a homogenous phase with particles uniformly sized. Moreover, it was observed that, these particles possessed nano-rod morphology with a length of 1.4μm and an average width of about 97nm. The FESEM micrograph (Figure 2b) of the sample obtained after hydrothermal treatment of the mixture of V_2O_5 and dodecylamine (V-DDA) showed that, the synthesized material was made of homogenous phase with uniform particles demonstrating nanotube morphology sizing about 76nm and 1.2μm in diameter and length, respectively. The morphology of the V_2O_5 nano-needles (V-A) was revealed in the FESEM image of the Figure 2c. The as-prepared products were composed of large quantities of one-dimensional V_2O_5 nano-needles with typical length of up to 3μm and the diameter of them varied in the range of 80-115nm. It was concluded from this figure that, the type of amine played an important role in controlling the morphologies of the V_2O_5 nanostructures. When the diethanolamine introduced, large amounts of flower-like V_2O_5 nanostructures (V-DEA) were obtained, as shown in Figure 2d. Moreover, the detailed morphology of these V_2O_5 nanoflowers revealed that, they possessed smooth surfaces.

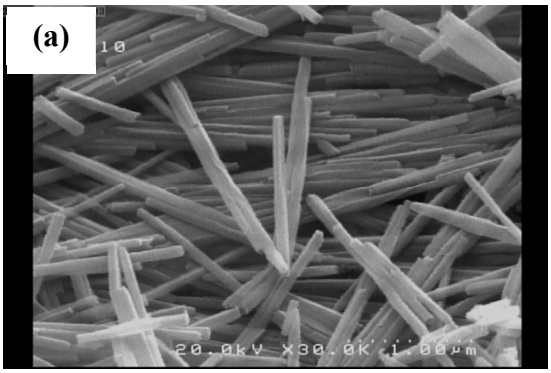

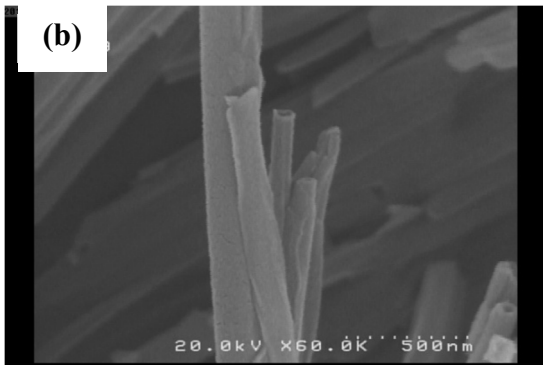

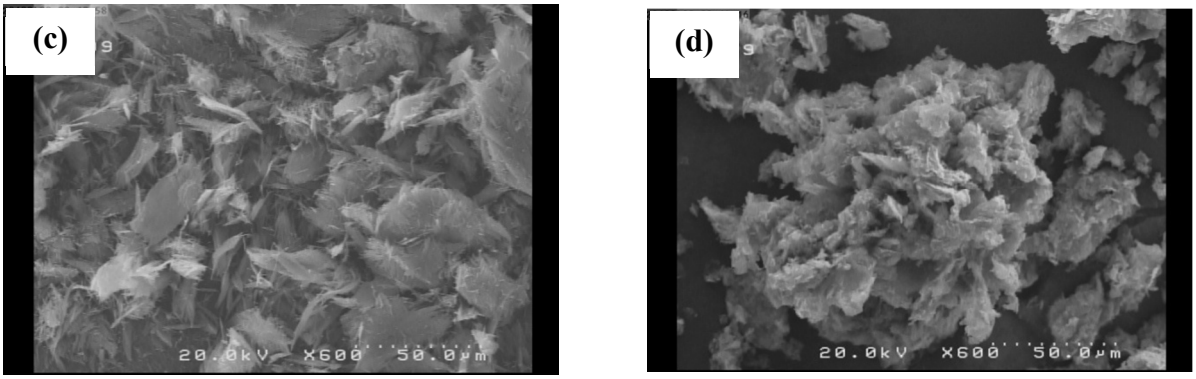

Figure 2: FESEM micrographs of: a) V-PA, b) V-DDA, c) V-A and d) V-DEA for differently prepared catalysts in this research

Huang et al. also pointed out that, organic molecules such as; surfactants had the ability to control the shape and size of the particles [23]. The dodecylamine played a critical role in such system due to the fact that; the tube-like morphologies might have not been obtained under the reflux and hydrothermal conditions in presence of other organic molecules like aniline or diethanolamine.

The morphology of the V_2O_5-graphene composite catalysts demonstrated in Figure 3. The composite texture hold an overall structure such that; the graphene sheets were stacked uniformly with V_2O_5 nanomaterial (designated as the V-PA-G) dispersed between them (Figure 3(a)). Noticeably, the resulting homogeneously entangled nature of these two components was the most critical feature substantially improving the performance of the composite catalysts. The FESEM images of various vanadium structures presented in Figures 3b to d also supported the uniform dispersion of V_2O_5 nanostructures within the graphene sheets leading to this homogeneous structure.

It was important to note that, the homogeneous mixing of components was previously ascribed to the graphene's acting as a surfactant [24,25]. This factor enhanced its ability to assist the dispersion of vanadium components in the solution as well as in a medium for the vanadium growth. Moreover, for the case of the pristine V_2O_5 nanostructure, they were vulnerable to agglomeration into clusters for sizes up to hundreds of nanometers due to the Ostwald ripening phenomenon during the calcination step. This emphasized the crucial role of the graphene sheets for good dispersion of the vanadium nanostructure.

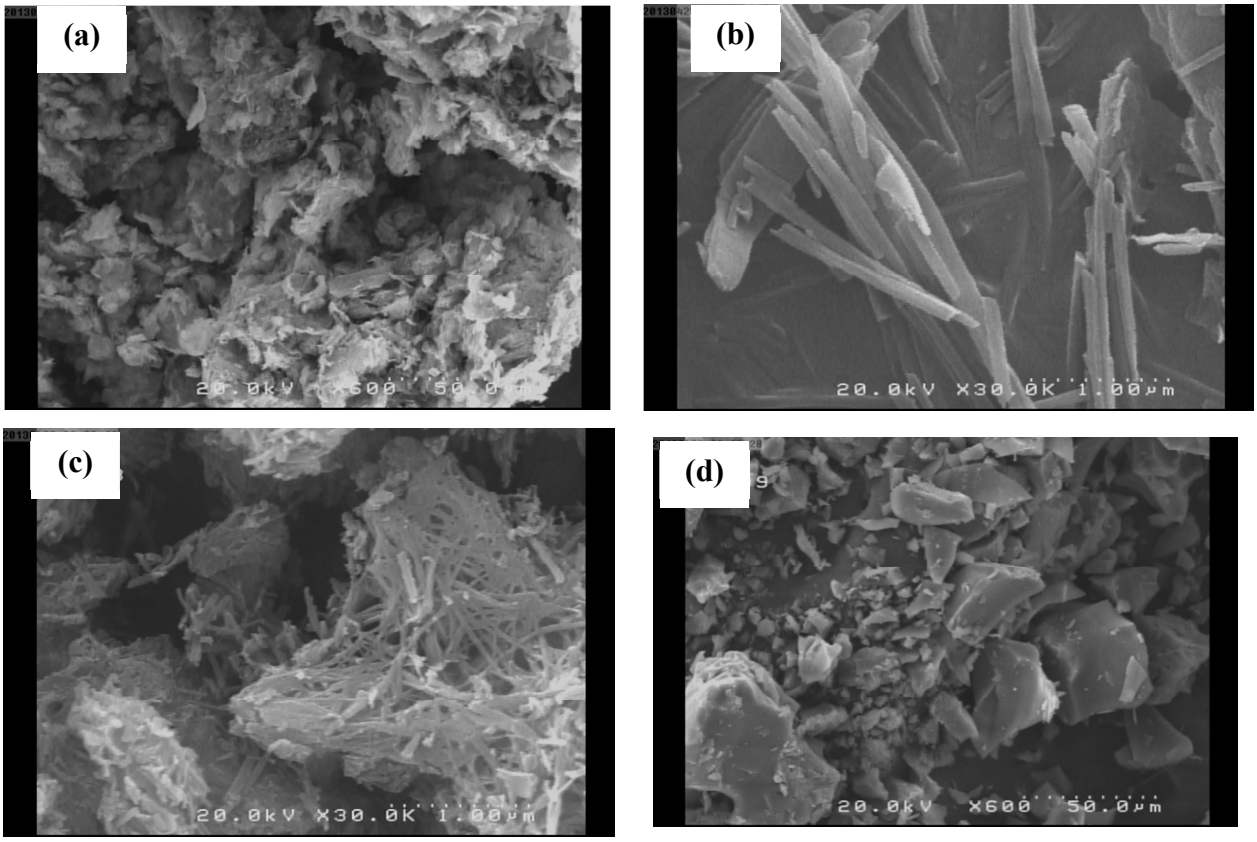

Figure 3: FESEM images of: a) V-PA-G, b) V-DDA-G, c) V-A-G and d) V-DEA-G for differently prepared catalysts in this study

3.2. XRD patterns

The crystallinity of the synthesized samples was examined by the XRD method. The obtained patterns of the VO_x-nanostructures via reflux and hydrothermal treatments of the V_2O_5 and propylamine, dodecylamine and aniline (Figure 4a) showed low angles reflection peaks characteristics of well-order layered structure. These behaviors also might have been due to the remaining organic templates in the system. This issue was further supported through other characterization techniques including the; FTIR and UV-vis spectroscopy to be discussed shortly. Peaks with highest intensity at the low diffraction angles reflected the distance between the vanadium oxide layers. This indicated that, the propylamine, dodecylamine and aniline molecules were indeed inserted between the vanadium oxide layers. The average distance between the parallel VO_x layers in the rod, tube and needle walls gave rise to certain reflections in reciprocal space. As a result, strong reflections at low diffraction angle appeared in the XRD pattern (Figure 4a). The organic template was incorporated between these VO_x layers. The XRD

pattern of the VO_x-NTs displayed two series of reflections: a 00l set with high intensity corresponding to the stacking of the layers along a direction perpendicular to the substrate and a hk0 set of reflections with lower intensity corresponding to the two dimensional structure of the layers. The 00l series provided the distance between the vanadium oxide layers. However, the synthesized VO_x nano-rod, -tube and -needle types apparently possessed a considerable stability compared to that of the aliphatic VO_x nanotubes. Moreover, it was previously demonstrated that, intercalated long chain alkylamines laid perpendicular to the oxide planes and the basal distance were close to the length of the amine [26].

The XRD patterns in the Figure 4(a) showed the powder diffraction patterns of the samples obtained after hydrothermal treatment of the V_2O_5 and diethanolamine, respectively. These patterns indicated that, all obtained diffraction peaks were identical to those of the VO_2(B) (according to the JCPDS card#81-2392). No peaks of any other phases or impurities were detected due to these patterns. This further indicated that a VO_2(B) phase with high purity might be obtained via the hydrothermal treatment at 180^oC using the crystalline V_2O_5 and diethanolamine as the sources of vanadium and reducing agent, respectively. The XRD pattern of the product was typical of a layered compound. It displayed two series of reflections including the; 001 and hk0 sets as discussed above.

Figure 4(b) showed the XRD patterns of vanadium oxide and amines hybridized with graphene. As demonstrated, all peaks were identified as V_8C_7 (PDF Card No. JCPDS #19-1394). This suggested that, at a given hydrothermal condition of high pressure and temperature, different amines, V_2O_5 and graphene might have gone through some reactions. In other words, carbon was obtained by the decomposition reaction of amines and then reacted with V_2O_5. During reducing reaction of carbon, the vanadium oxide was transformed to vanadium carbide [27].

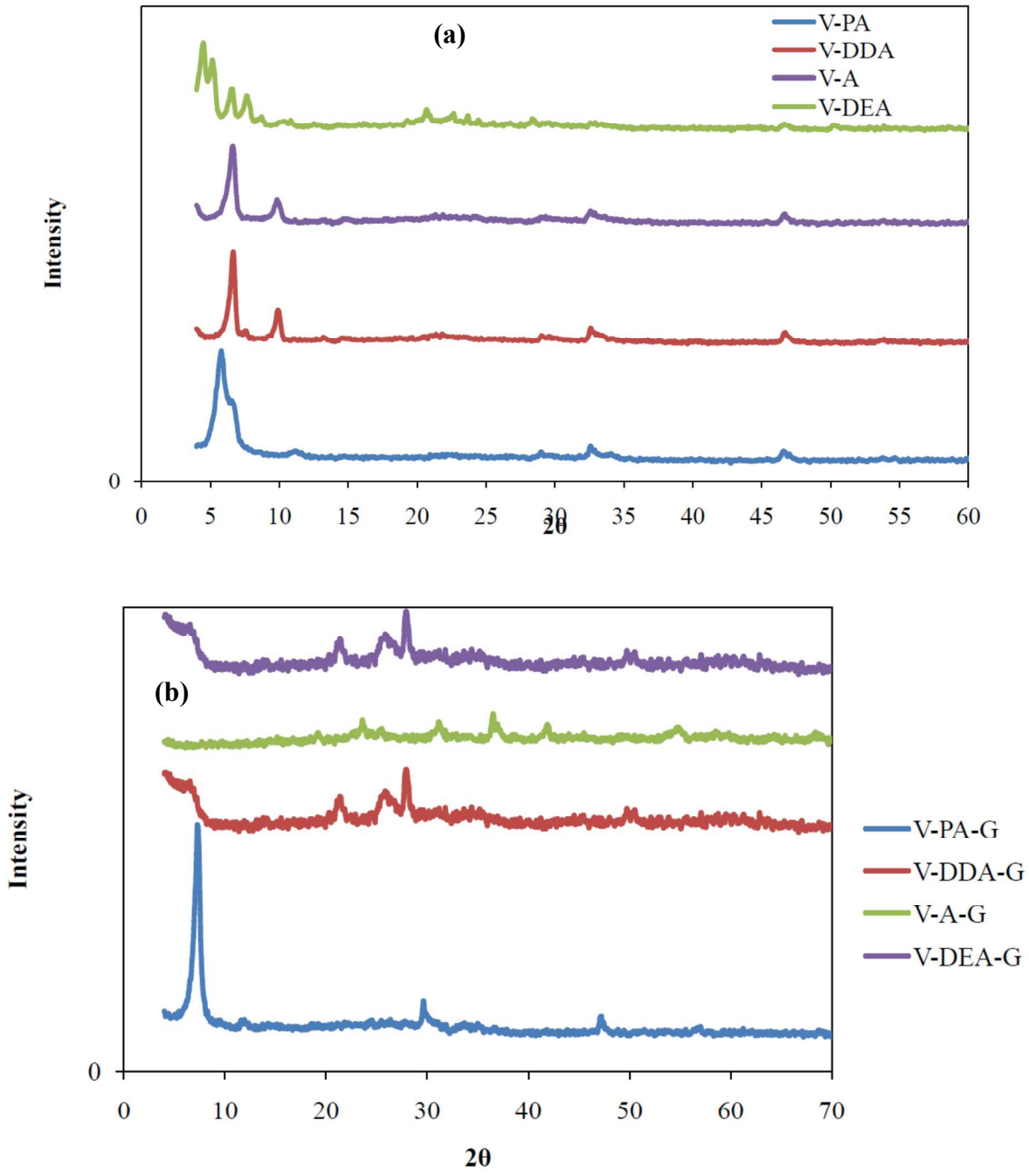

Figure 4: XRD patterns of a) different vanadium nanostructures and b) vanadium over graphene template for differently prepared catalysts

3.3. Thermal analysis

Thermal Gravimetric Analysis (TGA) and its differentiating curves for V-PA and V-DDA exhibited in Figure 5. In parts (a) and (c) of this figure being related to the V-PA species, a broad

peak in the temperature range of 50-100°C associated with a decrease in weight of about 2.64% (TGA) occurred. This was assigned to desorption of water molecules. A weight loss of ~14.16% occurred between 150 and 400°C. This was associated with an exothermic peak corresponding to the decomposition of residual organic molecules. Yet, another exothermic process with a weight increase of ~3.44% observed at 460°C. It corresponded to the oxidation of V^{4+} leading to the formation of the yellow V_2O_5 species according to the following reaction:

$$2VO_2 + 0.5O_2 \longrightarrow V_2O_5 \quad (9)$$

Figures 5b and d showed the TGA-DTGA curves of the V-DDA catalyst. The DTGA curve exhibited a broad endothermic peak between the room temperature and up to 100°C attributed to the adsorption of water molecules. A weak weight loss occurred between 150 and 400°C. It corresponded to the decomposition of residual organic molecules. Another endothermic process with a weight loss of 17.44% observed around 410 to 520°C, ascribed to the oxidation of V^{4+} leading to the formation of the yellow V_2O_5. TGA-DTGA curves of the synthesized vanadium oxide nanostructures over graphene presented in Figure 6. The TGA curve for V-DDA-G exhibited an exothermic peak around 100°C associated with a decrease in weight of 1.74% (TGA). The DTGA peak around 200°C corresponding to its TGA curves displayed a decrease of about 4.72%. This phenomenon was attributed to the combustion of organic molecules adsorbed at the surface. A weight loss of ~9.53% occurred between 300 and 400°C. It was associated with a sharp exothermic peak corresponding to the decomposition of organic molecules. Furthermore, there was an exothermic peak between 400 to 570°C with a weight decrease of 23.41% assigned to the crystallization of the yellow V_2O_5 species. The TGA curve for V-A-G exhibited an exothermic peak around 530°C corresponding to the crystallization of the V_2O_5. A weight loss of about 14.80% for this material was also observed.

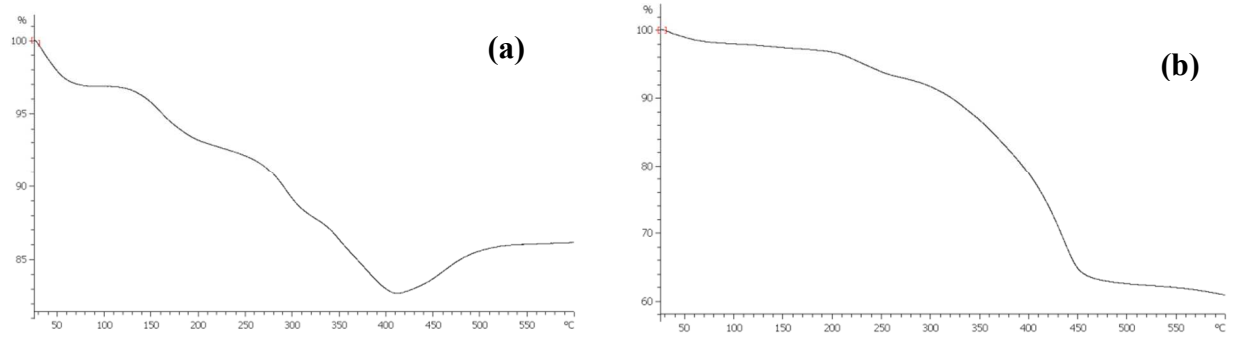

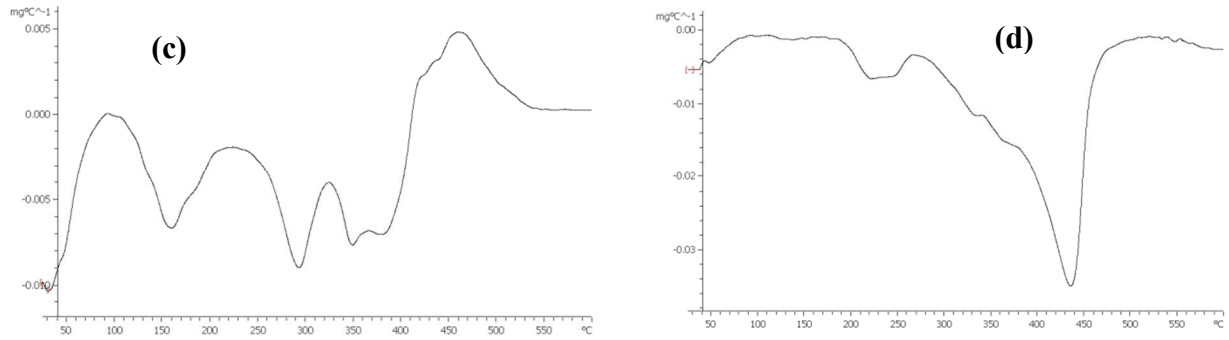

Figure 5: Thermal analysis including TGA for: a) V-PA and b) V-DDA as well as; DTGA for: c) V-PA and d) V-DDA materials

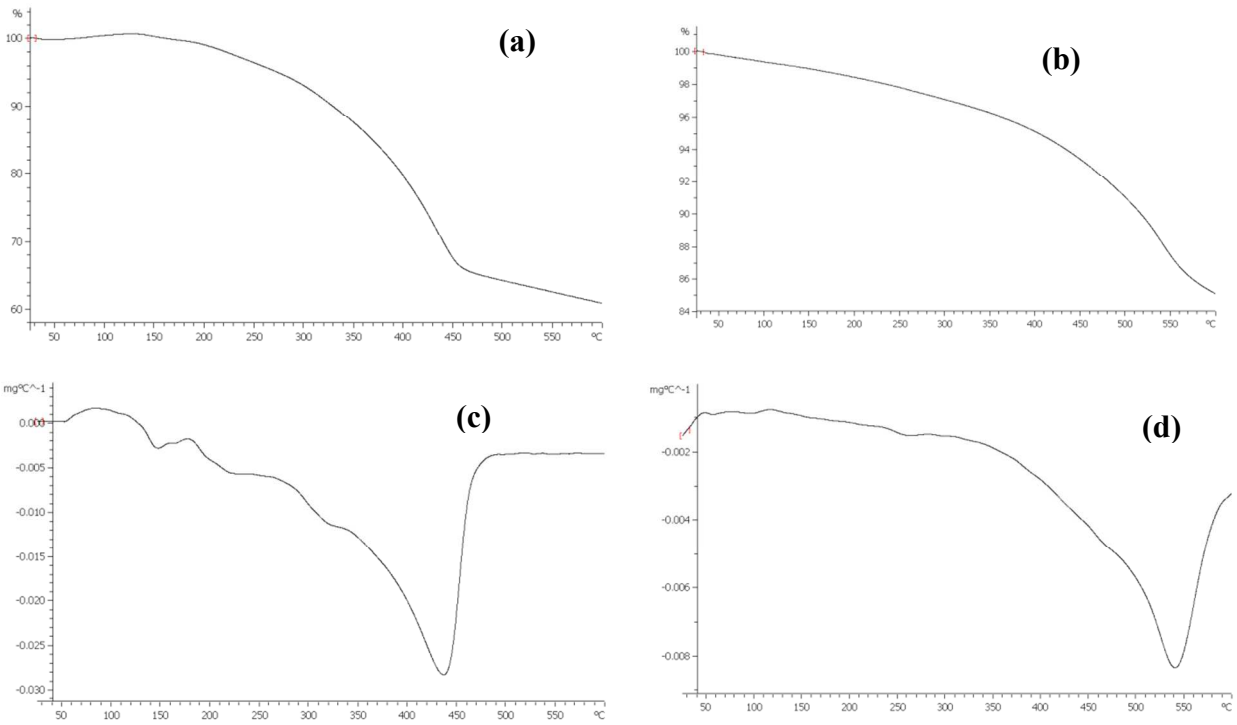

Figure 6: Thermal analysis including TGA for: a) V-DDA-G and b) V-A-G as well as; DTGA for: c) V-DDA-G and d) V-A-G materials

3.4. BET surface area

The specific surface area (S_{BET}), pore volume (V_{por}) and average pore size (d_{por}) of V_2O_5 nanostructures were measured by physisorption of nitrogen according to the BET method. The obtained results for different catalysts presented in Table 1. Analysis of the experimental findings provided important values of the specific surface area, pore volume and average pore

size of the considered materials. On the other hand, Figure 7 exhibited a type-IV N_2 adsorption/desorption isotherms being characteristic of mesoporous materials with a high energy of adsorption and the BJH pore size distribution for the V-A catalyst. The H_3-type hysteresis loops were usually observed with rigid bulk particles having uniform sizes [28]. This result confirmed by the specific surface area and the average pore size values for the aforementioned catalyst. The BJH part of the Figure 7 suggested that, the catalyst was hierarchically porous. Such a hierarchical structure was essential to ensure a good catalytic performance since the large pore channels allowed rapid mass transport of reactants and products while the small ones in combination with higher surface areas provided more surface active sites. It is noteworthy to mention that, Figure 7 was typical of the results for the prepared nanocatalysts provided in Table 1.

Table 1: Results of S_{BET}, V_{pore} and d_{pore} for different catalysts in this research

Catalysts	S_{BET} (m^2g^{-1})	V_{pore} (cm^3g^{-1})	d_{pore} (A°)
V-DDA	45.7	194.4×10^{-3}	190.29
V-DDA-G	78.2	$209.\ 1\times10^{-3}$	198.56
V-A	39.9	188.5×10^{-3}	189.15
V-A-G	84.6	218.2×10^{-3}	197.24

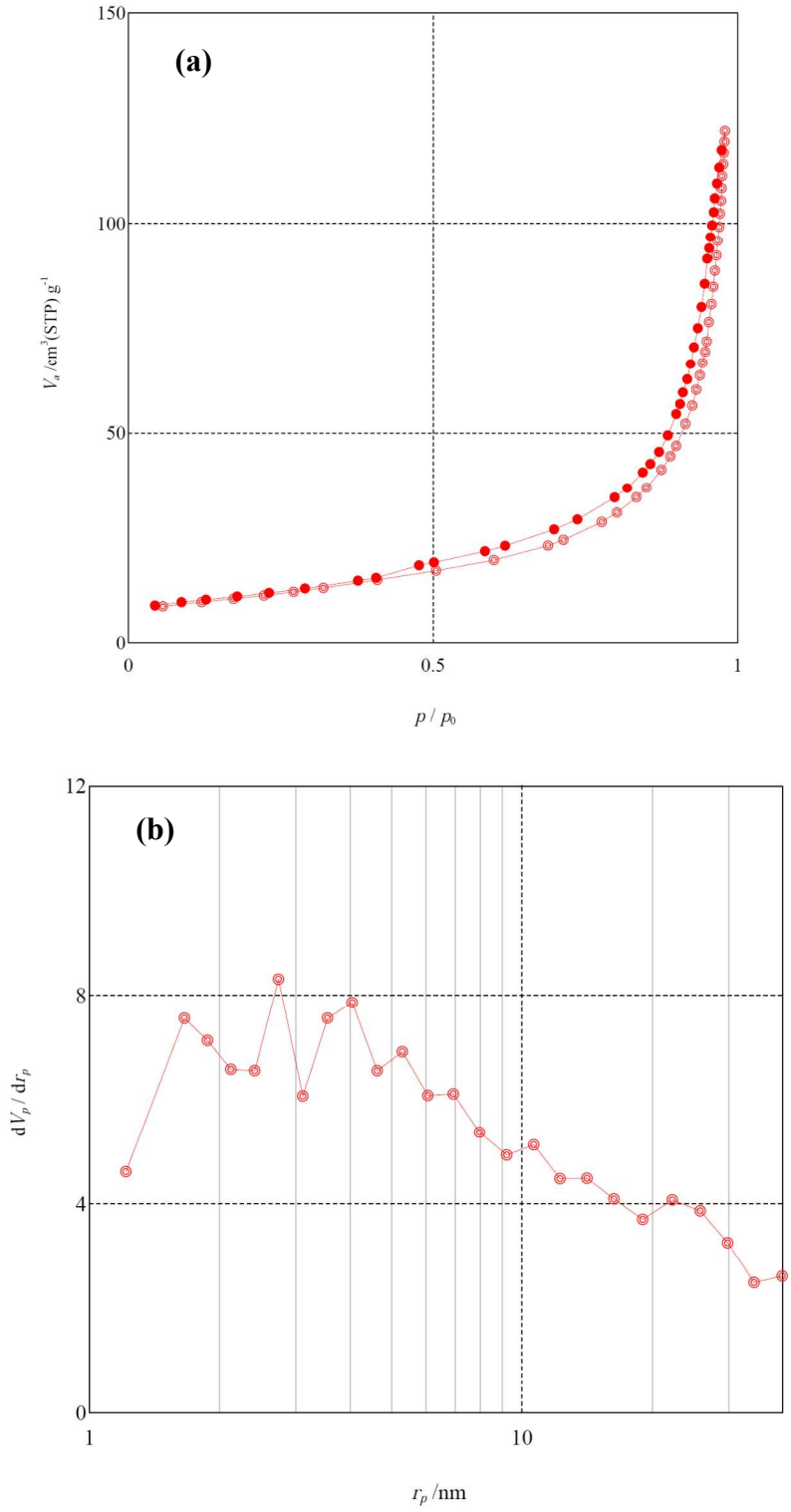

Figure 7: N_2 adsorption/desorption isotherm and BJH pore size distribution for the V-A nanocatalyst

3.5. FTIR analysis

Figure 8 displayed the FTIR spectra for the synthesized nanocatalysts. The band around 1000cm^{-1} observed for the vanadium nanostructures was present in many vanadium oxide compounds with intermediate oxidation state between V^{5+} and V^{4+} (Figure 8a). This was attributed to the stretching of short V=O bonds also present in the VO_2(B) species [29], while the band at 940cm^{-1}was attributed to the coupled vibration between V=O and V-O-V for all vanadium nanostructures except V-A catalyst. The vibrational band around 520-600cm^{-1}was attributed to the V-O-V octahedral bending modes. These characterizations suggested a model for the formation of nanorods or nanotubes. To the best of these authors' knowledge and experiences, the whole formation process of the VO_2(B) nanorods under reflux followed by hydrothermal conditions might have been expressed through Figure 8(a). To explain the mechanism controlling the morphology of the product after the hydrothermal treatment, a possible intermediate process was suggested on the basis of the lamellar structure of the precursors [30]. Since this structure was stabilized by the dodecylamine molecules, it was reasonable that the lamellate structure would break down after displacement of the amine compounds. During the hydrothermal treatment, it was probable that the lamellar precursors would split into nanotubes, and the products obtained showed striated morphologies. However, in the hydrothermal synthesis, the lamellar intermediate product would split later in small stems because of the loss of dodecylamine molecules. The hydrophobic character of diethanolamine molecules made the immobilization of this lamellar structure difficult resulting in the collapse of the final lamellar precursor. This supported the exfoliation of the precursor and the formation of vanadium oxide nanoflowers. The benzylamine played a dual role as a reducing and structuring agent in the formation of nanotube materials. The FTIR spectrum of VO_x nanotubes and nanorods (Figure8a) revealed adsorptions at around 2900, 2850 and 1500cm^{-1} assigned to the stretching and bending modes of the different C-H vibrations in the propylamine and dodecylamine templates, respectively. At the vanadium and diethanolamine template sample the very likely adsorption band around 3500cm^{-1} belonged to the O-H vibrations expected to spread somehow around 3600cm^{-1} [28] depending on the strength of the hydrogen bonds. The signals between 500 and 1000cm^{-1} in VO_x nano-rods, -tubes and -needles attributed to various (group) vibrations of the V-O type [31]. The possible mechanism of nanotube formation was already presented in the open literature [26]. Moreover, in the course of the hydrothermal treatment, the lamellar structure

intercalated through amines through which the vanadium oxide sheets might start to bend at both ends of the layers at the same time. The bending sheets have the possibility to close perfectly leading to concentric cylinders. Figure 8(b) showed the FTIR spectra of vanadium oxide over graphene with amines as the templates. The broad band at around 530cm^{-1} for the V-DDA-G and V-DEA-G assigned to the V-O-V octahedral bending modes. The band at 950cm^{-1} associated with the stretching of short V=O bonds. The band appeared at 1050cm^{-1} was due to initial disorder from VO_2(B) octahedral arrangement. The absorption band at 3400cm^{-1} was due to the O-H functional group in the structure [32]. In the V-A-G spectra, the band in the vicinity of 500cm^{-1} attributed to the V-O-V octahedral bending mode ascribed to the vanadium in the structure. The somewhat of a plateau observed in the V-A-G sample was assigned to the carbon due to graphene in structure of the catalyst.

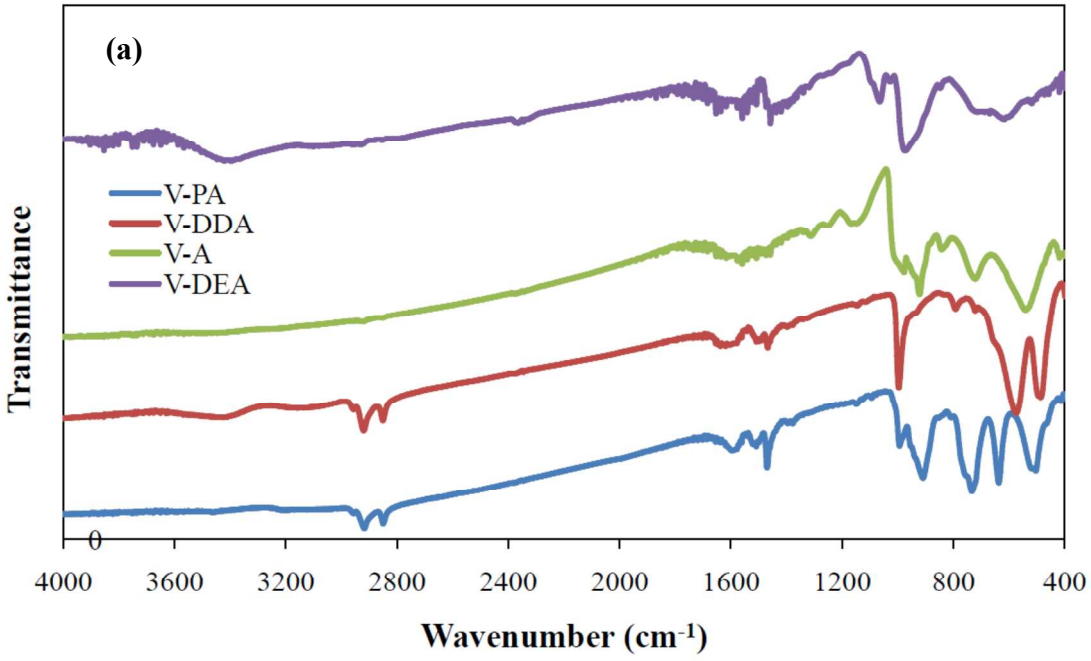

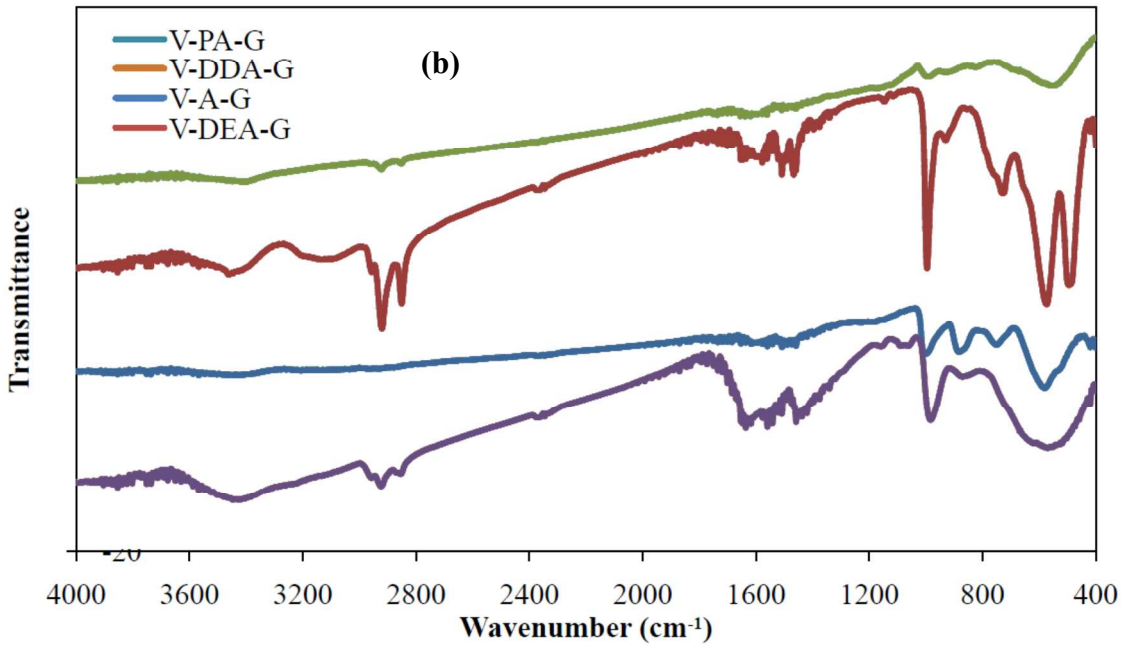

Figure 8: FTIR spectra of vanadium nanostructures (a) and vanadium over graphene (b) prepared through various amine nanocatalysts

3.6. UV-vis diffuse reflectance

UV-vis spectra provided useful information about structure and characteristics of the vanadium species understudied. The diffuse spectra for vanadium oxide nanostructures and that over graphene were presented in Figure 9. These spectra of the materials suggested that, the more ordered structures of vanadium as well as that, over graphene were due to greater retention of carbon rings in the basal planes. For all materials, a similar shoulder around 300nm was observed and attributed to $n \rightarrow \pi^*$ transitions of the carbonyl groups. All of these materials demonstrated a very similar behavior in terms of absorption wavelengths being placed in the vicinity of 225nm as previously reported for the graphene oxide [33].

On the other hand, the vanadium nanocatalysts had the absorption band in the visible region of the spectra. In the UV-region a strong ligand to metal charge transfer (LMCT) band due to the $O \rightarrow V^{5+}$ transition was observed around 290nm. The absence of absorption bands around 600-800nm indicated the absence of the d-d transitions due to VO^{2+} species. The UV spectrum for graphene containing samples showed peaks at around 300nm corresponding to the excitation of the π-plasmon of the graphitic structure.

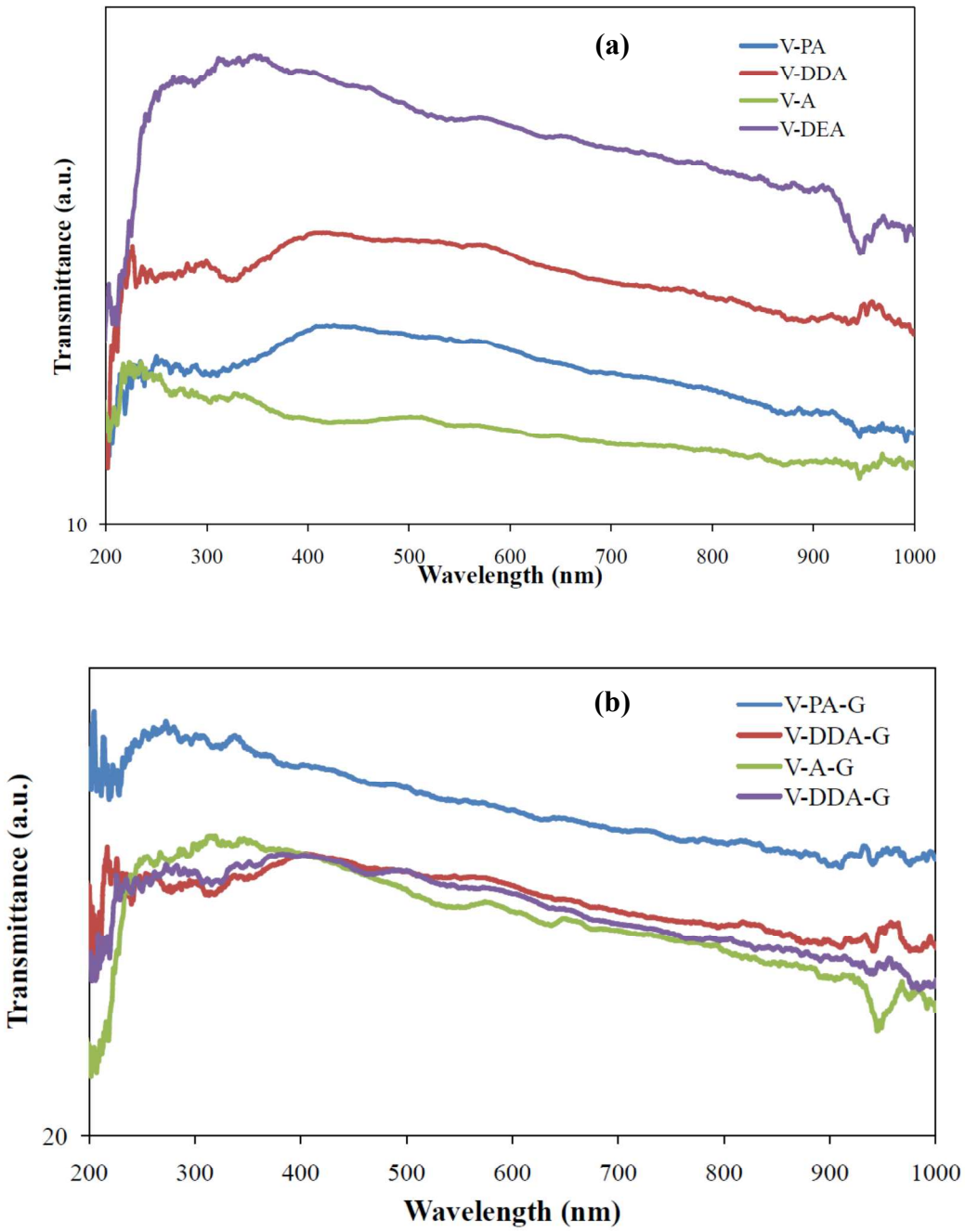

Figure 9: UV-vis spectra of (a) vanadium nanostructures and (b) vanadium over graphene through various amines prepared

4. Reactor performance evaluations

All physiochemical characterizations performed up to this point directed toward the fact that, the prepared pristine vanadium nanostructures via different amines (as the templates) resulted in different morphologies. Moreover, various bulk vanadium nanomaterials indicated by the V-PA and V-DDA revealed superior morphologies due to layered structures as well as no sign of any impurities detected for them. These made them the best candidates for the ODHP reaction. Besides, several vanadium nanostructures prepared over graphene (via the amines) resulted in uniform morphologies amongst which the vanadium over graphene with dodecylamine and aniline (*i.e.*, V-DDA-G and V-A-G) seemed to possess greater potentials for the propylene production. Therefore, reactor tests were needed to further determine which one of these so called better materials might be more desirable for catalyzing the reaction at hand.

GC analysis revealed that, the product mixture comprised of propylene, ethylene, CO, CO_2 and residual reactants resulting in carbon balance of almost 100%. It is noteworthy that, the carbon balance for all catalytic tests were performed and found to be within ±0.5% accuracy. No organic oxygenate was detected by the GC meaning that, more than 99.5% selectivities toward the aforementioned products was obtained. It is reminded that, at the understudied temperature in this research a very minute amount of methane might have been formed. This rationalized the exclusion of such species towards the carbon balance determinations. It was also shown through the open literature that, for the propane dehydrogenation [7], the selectivity towards methane was below 0.3% emphasizing the rational of this discussion. It is worth mentioning that, the vanadium oxide catalysts have resulted in the best yields towards the propylene via the ODHP reaction, although with an appropriate propylene amount [34]. In this venue, investigations upon the VO_x-phase as well as support materials leading to the reaction while obtaining attractive propylene productivities were the main goals of the present research. Actually, the target in the light alkanes ODH field is to develop synthesis methods allowing dispersion of the V_2O_5 as 2D-oligomeric VO_x-species rather than the V_2O_5 nano particles. This was re-confirmed though other studies in the open literatures [34,35]. In other words, the sub-monolayer catalysis is indeed the approach to be followed for the light alkanes' ODH process.

For comparative study of catalytic performance, the eight nanocatalysts including; different vanadium nanostructures prepared via the reflux and hydrothermal methods as well as the vanadium nanostructure over graphene synthesized via the amines were evaluated at 450°C

under C_3H_8/Air molar ratio of 0.5 and the total feed flowrate of 60mL/min. Propane conversion, propylene, ethylene and CO_x selectivities and yield of propylene for the vanadium oxide nanostructures over graphene at the end of the run (*i.e.*, after 6h from propane injection) were presented in Figure 10. These were for the catalytic ODHP reaction under the aforementioned operating conditions.

The stability of the current catalysts in the present research for the duration of 6h (*i.e.*; for one complete cycle) after the propane injection was monitored. It followed a stable trend. Moreover, through previous work of these authors [14] over the carbon-based catalysts; trajectories checking stability trends were determined for the propane conversion, propylene, ethylene and CO_x selectivities as well as propylene yield with time-on-stream. Because of the total consumption of oxygen, it was concluded that, the CO_2 formation during the ODHP reaction was mainly originated from oxidation of the hydrocarbon feedstock and not from burning of the carbon catalysts indicating occurrence of the consecutive reactions.

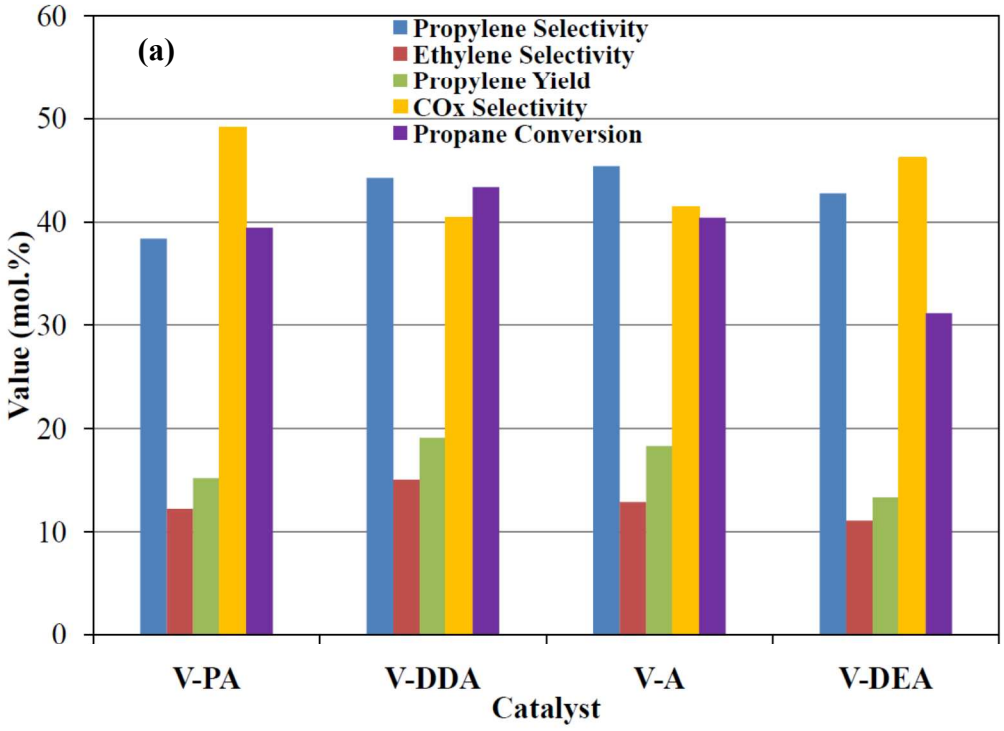

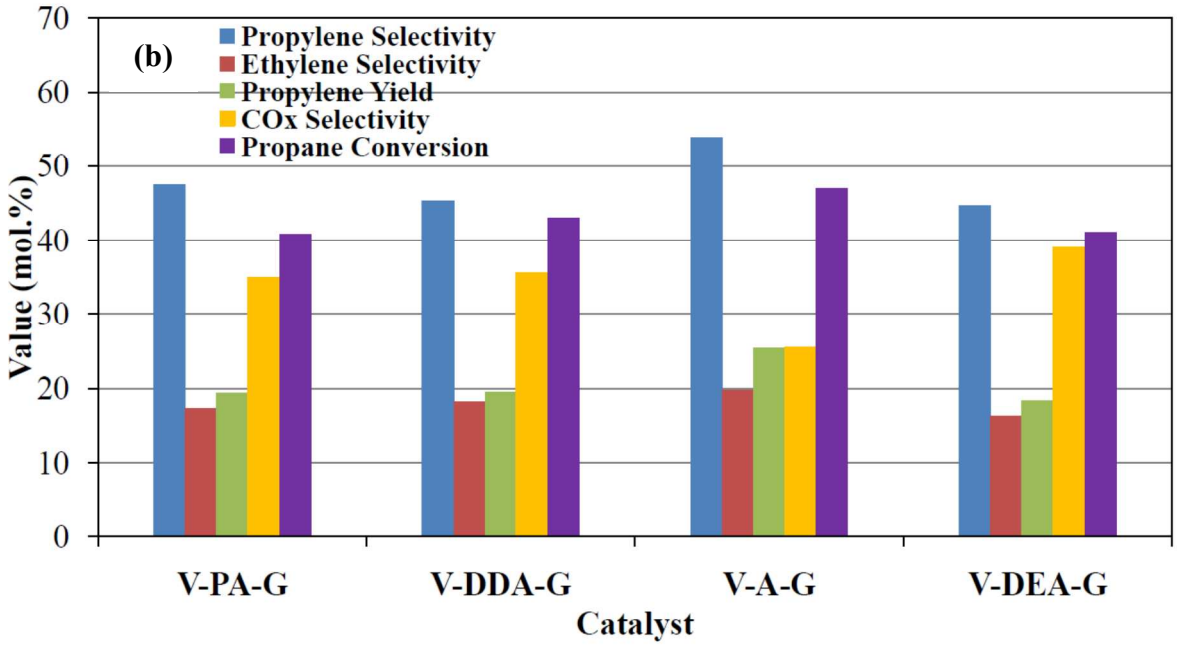

Figure 10: Propane conversion, product selectivities and yield of propylene over different a) vanadium oxide nanocatalysts, and b) vanadium oxide over graphene (under reaction conditions of T=450°C, C_3H_8/Air=0.5 and F_T= 60mL/min)

It was revealed that, V-A-G was an effective catalyst for the ODHP reaction since 53.93% propylene selectivity at 47.02% propane conversion was reached at 450°C. The propylene selectivity and propane conversion followed consistent trends emphasizing consecutive propylene degradation reactions took place. It was worthy to mention that, catalysts without calcination in air had a very low catalytic activity. This pointed out towards the issue that, the active sites for the ODHP (*i.e.*, carbonyl-like groups) were introduced on the carbon nanostructures through the air oxidation. Moreover, since both propane conversion and propylene selectivity were sensitive to the support structure compared with the dehydrogenation process, any impurities or inactive species on the support surface might have acted as a site diluent enhancing the selectivity towards dehydrogenation. This conclusion was also supported by Sui et al. [10]. Carbon support thus, acted as an inactive species and thereby improved propylene selectivity. The vanadium nanocatalysts prepared by reflux and hydrothermal methods incorporating different amines displayed the yields of 19.14% with the propane conversion and propylene selectivity of 43.32% and 44.18%, respectively for the V-DDA material. One ought to be careful that, when propane undergoes oxidative dehydrogenation to form propylene and

combustion of propane and propylene, the CO_x species formed should be accounted for. Carbon oxides might form both through oxidative reaction and steam-reforming of hydrocarbon feed and products. The selectivity toward the CO_x decreased on the catalysts containing graphene. Figure 10 indicated that, the vanadium with aniline based on graphene prepared by the reflux and hydrothermal methods resulted in a lower CO_x formation compared with other catalysts. Evaluations revealed that, vanadium over the graphene materials prepared by the hydrothermal method had a greater propylene yield and selectivity rendering those better choices of the optimum catalysts for the ODHP reaction.

Dissociative conversion of propane into propylene was observed under the abovementioned conditions. Considering the high stability of vanadium over graphene in air, it was a foregone conclusion that, the CO_x originated during the reaction mainly from oxidation of the hydrocarbon feedstock rather than from burning of the carbon catalysts. In order to investigate the effects of operating conditions on propylene formation, the temperature and feed molar ratio were undertaken as the more important choices of variables to be rationalized shortly. The range for operating variables investigated in the present research based on the values available in the open literature. The temperature range was chosen between 400 to 500°C. The rational for this choice was as follows. It was expected that, gasification of the CNTs and graphene might have become significant at temperatures above 530°C while the catalysts were inactive below 300°C [10]. The common range of molar feed ratio was between 0.3 to 0.8 while, effect of the feed flowrate due to the fine structure of catalysts was chosen at a common value of 60mL/min. Furthermore, the complete systematic optimization regarding the effect of operating parameters including the temperature, propane-to-air molar ratio as well as total feed flowrate upon the propane conversion, propylene, ethylene, and CO_x selectivities were performed through experimental design approach in a previous publication of these authors [14]. In that study, results of the experimental design for the catalyst evaluations indicated that the propane conversions and product selectivities were more influenced by the temperature and propane-to-air ratio than the feed flowrate. Moreover, optimum conditions for maximizing propane conversion and propylene selectivity as well as minimizing the CO_x selectivity were determined at the temperature of 500°C, propane-to-air molar ratio of 0.28 and total flowrate of 60mL/min [14]. In the present research however, the total feed flowrate kept constant at the optimized 60mL/min while effects of the other operating parameters investigated. In addition, to differentiate the thermal

dehydrogenation (*i.e.*; cracking) from the catalytic route for the ODHP reaction, reactor tests were performed on the propane feed without oxygen and in the absence of catalyst under which, the maximum propane conversion of 5% at 500°C was obtained. As such, it was safely concluded that, contributions of the thermal cracking and the catalytic ODHP reactions were distinguished from one another.

Figures 11 and 12 demonstrated the ODHP activity of V-DDA and V-A-G catalysts as a function of reaction temperature and propane-to-air ratio. It was revealed that, conversion enhanced as the reaction temperature increased while the selectivity for total olefins upgraded as well. Conversion values decreased upon increasing of the propane-to-air ratio from 0.3 to 0.8 at the same reaction temperature. All the catalysts had almost the same selectivity for alkenes as the concentration of air was doubled. As shown in Figure 12, amounts of the olefins obtained on the graphene based catalyst were higher than those of the V-DDA material.

Interaction of propane with oxygen-treated surfaces of the carbon catalysts was important to the yield of alkenes such as; ethylene and propylene. Propane molecules were activated by the surface oxygen groups to yield alkenes with remarkable selectivity. The surface of carbon materials was terminated by a variety of functionalized oxygen groups [10,36]. In these surface species, ketonic groups had great potential to coordinate a redox process due to being rich in electrons. On the other hand, production of the corresponding alkenes attributed to the Lewis basic sites known to abstract hydrogen atoms from the C-H bonds of alkanes. The reaction between the gas-phase oxygen and the abstracted hydrogen thus; regenerated the active sites accompanied by the formation of water [36,37]. This active site regeneration also enhanced the catalytic stability of such materials.

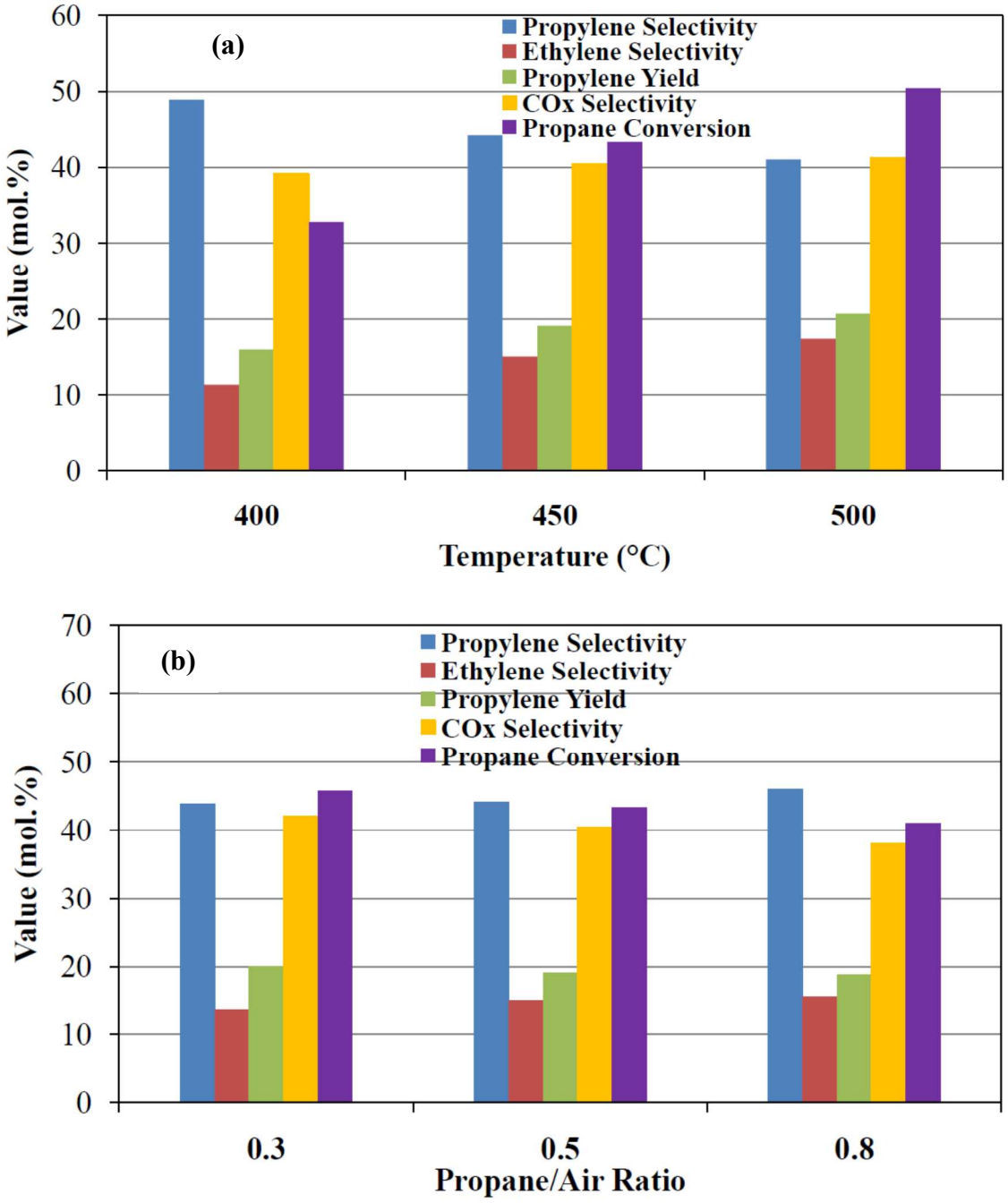

Figure 11: Effects of: a) reaction temperature at C_3H_8/Air molar ratio of 0.5 and b) C_3H_8/Air molar ration at T=450°C on olefin selectivities and propane conversion over the V-DDA catalyst

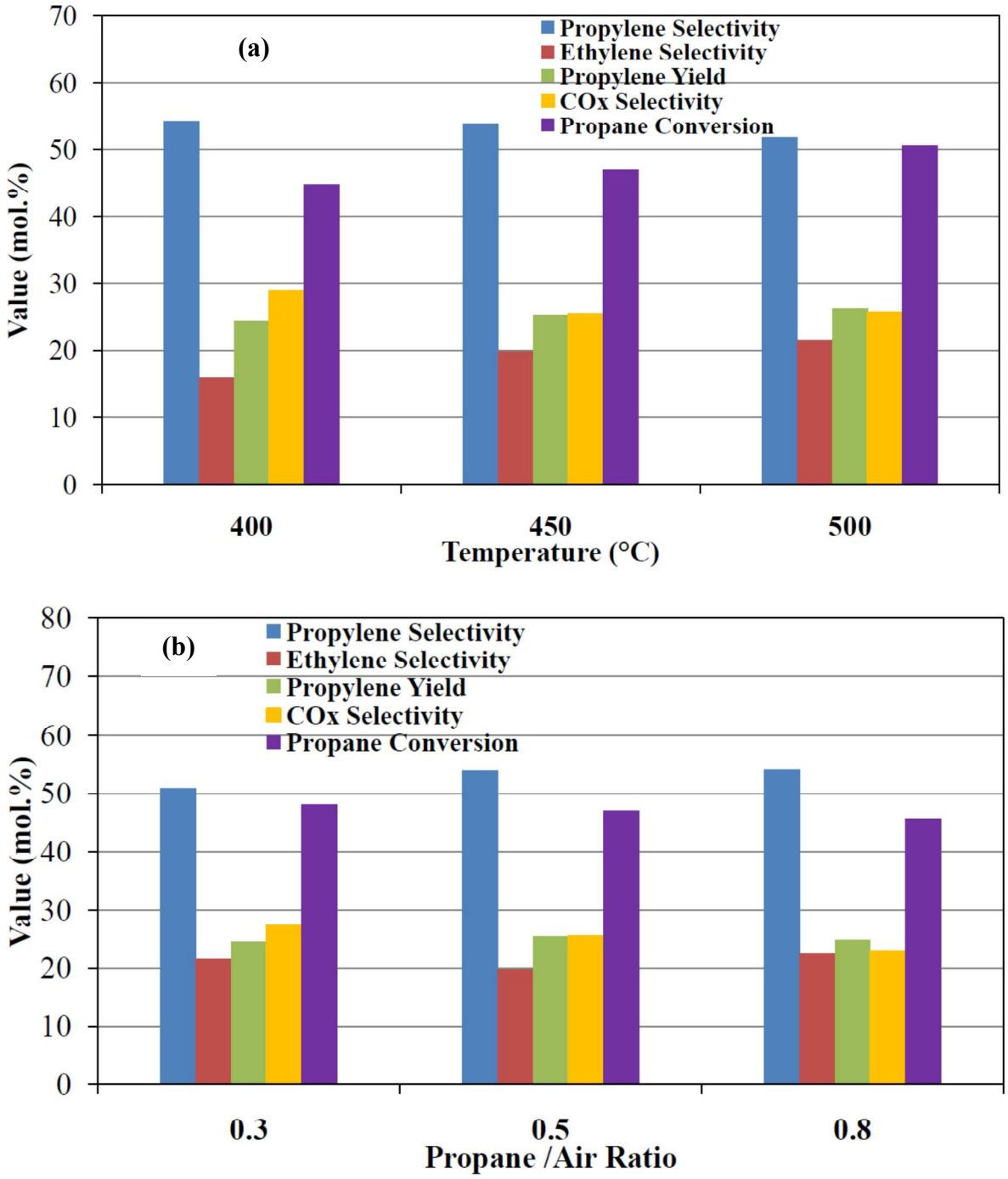

Figure 12: Effects of: a) reaction temperature at C_3H_8/Air molar ratio of 0.5 and b) C_3H_8/Air molar ration at T=450°C on olefin selectivities and propane conversion over the V-A-G material

Non-zero selectivity toward the CO_x species (both CO and CO_2) at close to zero values of not only conversion of propane but also selectivity of propylene revealed that, direct total oxidation

of propane to carbon oxides took place over catalysts understudied. This was further confirmed with the observation that, the propylene selectivity lowered with increasing propane conversion while the selectivity towards ethylene enhanced (*i.e.*; Figures 11a and 12a). This observation indicated that, both CO and CO_2 formed also via consecutive oxidation of propane and propylene as primary species. Selectivity toward the CO_x materials was more pronouncedly influenced by the degree of propane conversion upon changing of the propane to air ratio (see Figures 11b and 12b). Thus, it was concluded that, the propylene rather than propane was preferentially oxidized towards formation of the CO_x species.

In addition, it seemed that, a high reaction temperature and low C_3H_8/Air molar ratio favored higher propylene yields. Moreover, both such variables were benefitial for the carbon-based sturcture gasification of the V-A-G catalyst at tempreaturesbeyound 530°C. Nonetheless, limitations on such parameters restrained achieving higher propylene yield. Furthermore, the production of the CO_x led to lowering of the products selectivities indicating that, the reflux followed by the hydrothermal method increased the extent of the synthesized catalytic active sites.

Ultimately, the comparative reactor performance results of the best obtained catalysts for the ODHP reaction through this work with those of different materials available in the open literature were presented in Table 2. These results emphasized that, the synthesized catalysts in this research proved to be superior. It is clearly revealed through this table that, the catalysts utilized in the current study burned 50% of propane. On the other hand, to prove the stability and ideality of the graphene support for this purpose, a previous study performed the reactor experiments at different residence times under differential conditions (*i.e.*; below 10% propane conversion). The results emphasized that, the graphene was indeed a very suitable support material for the propane ODH carried out on supported V_2O_5 catalysts [38]. Moreover, in a previous publication of these researchers [38] the application of the design of experiment (DOE) coupled with the artificial neural networks (ANN) led to a kinetic study of the ODHP over a vanadium-graphene catalyst at 400-500^{o}C. The proposed reaction network composed of consecutive and simultaneous reactions expressing the kinetics through simple power law equations involving a total of 20 unknown parameters determined through non-linear regression analysis. Due to the actual complex nature of the system from the main and side reactions point of view, such power law model was chosen instead of a more complicated mechanistic model to

realize the chemical kinetics behavior of the system. Nonetheless, the results of such kinetic modeling satisfactorily fit the experimental data. Moreover, the as-prepared catalysts [38] were extremely fine particles, so that intra-particle diffusion was neglected. Besides, under different feed flowrates of identical compositions the external mass transfer resistance was also negligible. The absence of temperature and concentration gradients both outside and inside of the catalyst particle as well as a series of classical empirical correlations employed to evaluate and emphasize the negligibility of the limiting conditions. These criteria guaranteed a well-established kinetic control regime of operation in that investigation [38]. With this background, these authors synthesized the new materials in the current paper as well as investigated them from process, performance and application point of views. In other words, no rate and kinetic modeling was undertaken in the current research. On the other hand, the kinetic investigations of vanadium over different supports were thoroughly investigated by the Carrero et al. [34,35].

It is noteworthy that, catalytic deactivation tests were not performed for the prepared catalysts as described earlier in the experimental section of this paper. Besides, the determined carbon balance revealed no considerable alteration (before and after the reactor tests) occurred emphasizing rather stable trends of catalysts' performance. Moreover, the goal of the present research was to investigate the feasibility of the newly synthesized catalyst from performance point of view. Nonetheless, in order to study the deactivation or structure of the synthesized catalyst, special characterizations such as; determination of the crystallite size of the corresponding materials (before and after the reactor tests) ought to be performed. Such issues indeed need to be addressed in order to further develop these catalysts.

Table 2: The comparative results of vanadium catalysts for the ODHP reaction

Catalyst/Oxidizing agent	**T (^{o}C)**	**Propane Conversion (%)**	**Selectivity (%)**			**C_3H_6 Yield (%)**	**Reference**
			C_2H_4	**C_3H_6**	**CO_x**		
6%V/6%Ti/SBA-15	500	1.1	-	88	-	0.97	35
4%V/13%Ti/SBA-15	500	1.8	-	81	-	1.46	35
V_2O_5/O_2	500	6.73	-	25.26	73.70	1.69	39
V_2O_5/N_2O	500	4.30	-	72.25	27.21	3.11	39
V_2O_5/Air	460	3.5	-	15.3	89.7	0.54	40
Al_2O_3/O_2 and H_2S	700	24.2	13.9	71.3	5.7	17.2	41
Al_2O_3/O_2	700	26.8	34.8	44.5	3.1	11.9	41
V-Al_2O_3/O_2 and H_2S	700	53.7	25.1	56.5	1.0	30.4	41
V-Al_2O_3/O_2	700	22.8	29.9	25.0	22.3	5.70	41
CeO_2	450	7.25	0.0	18.14	82.21	1.32	42
3.6V-SBA-15/O_2	540	13	-	60	37	7.80	43

3.6V-SBA-16/O_2	540	13	-	57	41	7.41	43
3.6V-MCM-48/O_2	540	13	-	56	42	7.28	43
V-DDA	500	50.44	17.44	41.03	41.28	20.69	Present work
V-A-G	500	50.65	21.49	51.86	25.75	26.27	Present work

5. Conclusions

In this research, several vanadium oxide nanostructures were prepared from a vanadium precursor and different amines. This was done through a reflux method followed by a hydrothermal treatment. Nano-rods, -tubes, -needles and -flowers of vanadium oxides successfully synthesized through the simple yet elegant hydrothermal process. This was performed utilizing a mixture of the crystalline V_2O_5 as the vanadium source and various amines including propylamine, dodecylamine, aniline and diethanolamine as the reducing agents along with structure-directing templates under mild operating conditions. It was shown that, the organic components played an important role in the texture and morphology of the final products. In fact, the bulk nanostructures in this study displayed high crystallinity enhancing the ODHP reaction. The prepared catalyst named V-DDA displayed the best activity and yield from conversion and selectivity viewpoints. Moreover, hybrid catalysts from the vanadium oxide along with the aforementioned amines and graphene as the template synthesized via the reflux followed by the hydrothermal process. The synthesized hybrid catalysts evaluated in the ODHP process utilizing the V-A-G catalysts displayed higher conversions and selectivities. All synthesized catalysts (*i.e.*, bulk and hybrid) were characterized through the FESEM, FTIR, XRD, TGA/DTA, UV-Vis and BET/BJH surface area methods and went through the aqueous phase reaction carried out under mild conditions. These as-synthesized materials revealed to be promising candidates for wide spread investigations of the ODHP reaction. Ultimately, the current investigations over different vanadium-based and vanadium over graphene catalysts led to desirable and challenging materials providing high propylene production while minimizing the CO_x formation.

References

[1] Bijan Barghi, Moslem Fattahi, Farhad Khorasheh, Kinetic modeling of propane dehydrogenation over an industrial catalyst in the presence of oxygenated compounds, Reaction Kinetics, Mechanisms and Catalysis 107 (1) (2012) 141-155

[2] Sameer A. Al-Ghamdi, Hugo I. de Lasa, Propylene production via propane oxidative dehydrogenation over VO_x/γ-Al_2O_3 catalyst, Fuel 128 (2014) 120-140

[3] Max Heinritz-Adrian, Sascha Wenzel, Fekry Youssef, Advanced propane dehydrogenation, Petroleum Technology Quarterly (PTQ) 13(1) (2008) 83, 85-86, 88, 91

[4] K. Buker, S. Donnermeyer, H. Gehrke, M. Heinritz-Adrian, STAR Process for the On-purpose Production of Propylene, Oil Gas European Magazine 36 (1) (2010) 40-44

[5] E.A. Mamedov, V. Cortes Corberan, Oxidative dehydrogenation of lower alkanes on vanadium oxide-based catalysts. The present state of the art and outlooks, Applied Catalysis A: General 127 (1-2) (1995) 1-40

[6] F. Arena, F. Frusteri, A. Parmaliana, Structure and dispersion of supported-vanadia catalysts. Influence of the oxide carrier, Applied Catalysis A: General 176 (2) (1999) 189-199

[7] A.H. Shahbazi Kootenaei, J. Towfighi, A. Khodadadi, Y. Mortazavi, Stability and catalytic performance of vanadia supported on nanostructured titania catalyst in oxidative dehydrogenation of propane, Applied Surface Science 289 (2014) 26-35

[8] G. Deo, I.E. Wachs, Effect of Additives on the Structure and Reactivity of the Surface Vanadium Oxide Phase in V_2O_5/TiO_2 Catalysts, Journal of Catalysis 146 (2) (1994) 335-345

[9] D.S. Su, N. Maksimova, J.J. Delgado, N. Keller, G. Mestl, M.J. Ledoux, R. Schlögl, Nanocarbons in selective oxidative dehydrogenation reaction, Catalysis Today 102-103 (2005) 110-114

[10] Zhi-jun Sui, Jing-hong Zhou, Ying-chun Dai, Wei-kang Yuan, Oxidative Dehydrogenation of Propane over Catalysts Based on Carbon Nanofibers, Catalysis Today 106 (2005) 90-94

[11] Xi Liu, Dang Sheng Su, Robert Schlögl, Oxidative dehydrogenation of 1-butene to butadiene over carbon nanotube catalysts, Carbon 46 (3) (2008) 547-549

[12] Gerhard Mestl, Nadezhda I. Maksimova, Nicolas Keller, Vladimir V. Roddatis, Robert Schlögl, Carbon Nanofilaments in Heterogeneous Catalysis: An Industrial Application for New Carbon Materials?, Angewandte Chemie International Edition 40 (11) (2001) 2066-2068

[13] Marc J Ledoux, Claude Crouzet, Cuong Pham-Huu, Vincent Turines, Kostantinos Kourtakis, Patrick L Mills, Jan J Lerou, High-Yield Butane to Maleic Anhydride Direct Oxidation on Vanadyl Pyrophosphate Supported on Heat-Conductive Materials: β-SiC, Si_3N_4, and BN, Journal of Catalysis 203 (2) (2001) 495-508

[14] Moslem Fattahi, Mohammad Kazemeini, Farhad Khorasheh, Ali Morad Rashidi, Vanadium Pentoxide Catalyst over Carbon-based Nanomaterials for the Oxidative Dehydrogenation of Propane, Industrial & Engineering Chemistry Research 52 (46) (2013) 16128-16141

[15] Liqiang Mai, Wen Chen, Qing Xu, Quanyao Zhu, Chunhua Han, Junfeng Peng, Cost-saving synthesis of vanadium oxide nanotubes, Solid State Communications 126 (10) (2003) 541-543

[16] Zeeshan Nawaz, Fei Wei, Light-alkane oxidative dehydrogenation to light olefins over platinum-based SAPO-34 zeolite-supported catalyst, Industrial and Engineering Chemistry Research 52 (1) (2013) 346-352

[17] J. Livage, Vanadium pentoxide gels, Chemistry of Materials 3 (4) (1991) 578-593

[18] Ping Liu, Igor L. Moudrakovski, Jun Liu, Abdelhamid Sayari, Mesostructured vanadium oxide containing dodecylamine, Chemistry of Materials 9 (1997) 2513-2520

[19] Thomas Chirayil, Peter Y. Zavalij, M. Stanley Whittingham, Hydrothermal synthesis of vanadium oxides, Chemistry of Materials 10 (10) (1998) 2629-2640

[20] Ahmad Ghozatloo, Mojtaba Shariaty-Niasar, Ali Morad Rashidi, Preparation of nanofluids from functionalized graphene by new alkaline method and study on the thermal conductivity and stability, International Communications in Heat and Mass Transfer 42 (2013) 89-94

[21] Razieh Jabari Seresht, Mohsen Jahanshahi, Alimorad Rashidi, Ali Asghar Ghoreyshi, Synthesize and characterization of Graphene nanosheets with high surface area and nano-porous structure, Applied Surface Science 276 (2013) 672-681

[22] L. Bouhedja, N. Steunou, J. Maquet, J. Livage, Synthesis of Polyoxovanadates from Aqueous Solutions, Journal of Solid State Chemistry 162 (2) (2001) 315-321

[23] Feng Huang, Hengzhong Zhang, Jillian F. Banfield, Two-Stage Crystal-Growth Kinetics Observed during Hydrothermal Coarsening of Nanocrystalline ZnS, Nano Letters 3 (3) (2003) 373-378

[24] Jung Woo Lee, Soo Yeon Lim, Hyung Mo Jeong, Tae Hoon Hwang, Jeung Ku Kang, Jang Wook Choi, Extremely stable cycling of ultra-thin V_2O_5 nanowire-graphene electrodes for lithium rechargeable battery cathodes, Energy Environmental Science 5 (2012) 9889-9894

[25] Jaemyung Kim, Laura J. Cote, Franklin Kim, Wa Yuan, Kenneth R. Shull, Jiaxing Huang, Graphene oxide sheets at interfaces, Journal of the American Society 132 (23) (2010) 8180-8186

[26] F. Sediri, N. Gharbi, From crystalline V_2O_5 to nanostructured vanadium oxides using aromatic amines as templates, Journal of Physics and Chemistry of Solids 68 (2007) 1821-1829

[27] Shu-fang Ma, Jian Liang, Jun-fu Zhao, Bing-she Xu, Synthesis, characterization and growth mechanism of flower-like vanadium carbide hierarchical nanocrystals, Cryst Eng Comm 12 (2010) 750-754

[28] K.S.W. Sing, D.H. Everett, R.A.W. Haul, L. Moscou, R.A. Pierotti, J. Rouquerol, T. Siemieniewska, Reporting physisorption data for gas/solid systems with special reference to the determination of surface area and porosity, Pure and Applied Chemistry 57 (4) (1985) 603-619

[29] J.-C. Valmalette, J.-R. Gavarri, High efficiency thermochromic VO_2(R) resulting from the irreversible transformation of VO_2(B), Materials Science and Engineering B 54 (3) (1998) 168-173

[30] Libo Li, Yadong Li, A simple model for growth of semiconductor nanorods using lamellar precursors, Materials Chemistry and Physics 94 (1) (2005) 1-6

[31] V.V. Fomichev, P.I. Ukrainskaya, T.M. Ilyin, Vibrational spectra and electrostatic fields of V_2O_5 and lithium vanadium bronzes, Spectrochimica Acta Part A: Molecular and Biomolecular Spectroscopy 53 (11) (1997) 1833-1837

[32] Ch.V. Subba Reddy, Edwin H. Walker Jr., S.A. Wicker Sr., Quinton L. Williams, Rajamohan R. Kalluru, Synthesis of VO_2(B) nanorods for Li battery application, Current Applied Physics 9 (6) (2009) 1195-1198

[33] X. Gao, J. Jang, H. Nagase, Hydrazine and Thermal Reduction of Graphene Oxide: Reaction Mechanisms, Product Structures, and Reaction Design, Journal of Physical Chemistry C 114 (2) (2010) 832-842

[34] Carlos A. Carrero, Christopher J. Keturakis, Andres Orrego, Reinhard Schomäcker, Israel E. Wachs, Anomalous reactivity of supported V_2O_5 nanoparticles for propane oxidative dehydrogenation: influence of the vanadium oxide precursor, Dalton Transactions 42 (2013) 12644-12653

[35] Carlos Carrero, Markus Kauer, Arne Dinse, Till Wolfram, Neil Hamilton, Annette Trunschke, Robert Schlögl, Reinhard Schomäcker, High performance $(VO_x)_n$-$(TiO_x)_m$/SBA-15 catalyst for the oxidative dehydrogenation of propane, Catalysis Science and Technology 4 (2014) 786-794

[36] Da Young Jang, Hyung Gyu Jang, Gye Ryung Kim, Geon-Joong Kim, Oxidative dehydrogenation of n-butane on nano-carbon catalysts having graphitic structures, Research on Chemical Intermediates 37 (9) (2011) 1145-1156

[37] Jian Zhang, Xi Liu, Raoul Blume, Aihua Zhang, Robert Schlögl, Dang Sheng Su, Surface-Modified Carbon Nanotubes Catalyze Oxidative Dehydrogenation of *n*-Butane, Science 322 (2008) 73-77

[38] Moslem Fattahi, Mohammad Kazemeini, Farhad Khorasheh, Ali Morad Rashidi, Kinetic modeling of oxidative dehydrogenation of propane (ODHP) over a vanadium-graphene catalyst: Application of the DOE and ANN methodologies, Journal of Industrial and Engineering Chemistry 20 (2014) 2236-2247

[39] Evgenii V. Kondratenko, Olga Ovsitser, Joerg Radnik, Matthias Schneider, Ralph Kraehnert, Uwe Dingerdissen, Influence of reaction conditions on catalyst composition andselective/non-selective reaction pathways of the ODP reaction over V_2O_3, VO_2 and V_2O_5 with O_2 and N_2O, Applied Catalysis A: General 319 (2007) 98-110

[40] L. Balderas-Tapia, I. Hernández-Pérez, P. Schacht, I.R. Córdova, G.G. Aguilar-Ríos, Influence of reducibility of vanadium-magnesium mixed oxides on the oxidative dehydrogenation of propane, Catalysis Today 107-108 (2005) 371-376

[41] Peter D. Clark, Norman I. Dowling, Xiangyun Long, Yingwei Li, Oxidative dehydrogenation of propane to propene in the presence of H_2S at short contact times, Journal of sulfur chemistry 25 (6) (2004) 381-387

[42] Shigeru Sugiyama, Yutaka Iizuka, Etsushi Nitta, Hiromu Hayashi, John B. Moffat, Role of Tetrachloromethane as a Gas-Phase Additive in the Oxidative Dehydrogenation of Propane over Cerium Oxide, Journal of Catalysis 189 (2000) 233-237

[43] Roman Bulánek, Alena Kalužová, Michal Setnička, Arnošt Zukal, Pavel Čičmanec, Jana Mayerová, Study of vanadium based mesoporous silicas for oxidative dehydrogenation of propane and n-butane, Catalysis Today 179 (2012) 149-158